Proc. Natl. Acad. Sci. USA
Vol. 90, pp. 11618–11622, December 1993
Medical Sciences

Osteoporosis induced in mice by overproduction of interleukin 4

(transgenic mice/osteoblasts/osteoclasts/lck promoter/osteopenia)

DAVID B. LEWIS[a,b,c], H. DENNY LIGGITT[d], ERIC L. EFFMANN[e,f], S. TIMOTHY MOTLEY[e,f], STEVEN L. TEITELBAUM[g], KARL J. JEPSEN[h], STEVEN A. GOLDSTEIN[h], JEFFREY BONADIO[i], JOAN CARPENTER[d], AND ROGER M. PERLMUTTER[b,j,k,l]

Departments of [a]Pediatrics, [b]Immunology, [d]Comparative Medicine, [e]Radiology, [j]Biochemistry, [k]Medicine, and [l]Howard Hughes Medical Institute, University of Washington, Seattle, WA 98195; [f]Department of Radiology, Children's Hospital and Medical Center, Seattle, WA 98105; [g]Department of Pathology, Washington University, St. Louis, MO 63178; and [h]Orthopaedic Research Laboratory and [i]Department of Pathology, University of Michigan, Ann Arbor, MI 48109

Communicated by Robert H. Wasserman, August 23, 1993 (received for review June 8, 1993)

ABSTRACT **Osteoporosis is a common disease in which loss of bone mass results in skeletal fragility. The development of therapies for this disorder has been hampered by the lack of a convenient animal model. Here we describe a disorder in bone homeostasis in transgenic mice that inappropriately express the cytokine interleukin 4 (IL-4) under the direction of the lymphocyte-specific proximal promoter for the *lck* gene. Bone disease in *lck*–IL-4 mice appeared to result from markedly decreased bone formation by osteoblasts, features strikingly similar to those observed in cases of severe low-turnover human involutional osteoporosis. By 2 months of age, female and male *lck*–IL-4 mice invariably developed severe osteoporosis of both cortical and trabecular bone. Osteoporosis was observed in two independently derived founder animals, indicating that this phenotype was directly mediated by the IL-4 transgene.**

Maintaining skeletal bone mass is a dynamic process requiring a balance between bone resorption and formation (1). After the completion of skeletal growth, involutional osteoporosis may occur if bone resorption by osteoclasts (e.g., as occurs during remodeling) exceeds bone production by osteoblasts (2). Increased osteoclast activity and/or decreased osteoblast activity may contribute to the development of osteoporosis. Although involutional osteoporosis is a major cause of morbidity and mortality in developed countries (3), many issues regarding its pathogenesis and treatment remain unresolved.

A role for cytokines in the pathogenesis of osteoporosis has been proposed since interleukin 1, interleukin 6, and tumor necrosis factor α enhance bone resorption *in vitro* (4–6). The loss of estrogen production at the menopause accelerates osteoporosis in women, and it is intriguing that estrogen depletion by oophorectomy in mice causes an interleukin 6-dependent increase in trabecular bone osteoclasts (7). The amount of interleukin 1 and tumor necrosis factor α produced by circulating mononuclear cells may also increase after oophorectomy in humans (8, 9). Nevertheless, no direct evidence links increased production of these or other cytokines to the development of osteoporosis.

Interleukin 4 (IL-4) is a cytokine with pleiotropic effects on a wide variety of cell types (10). We have reported (11) the generation of transgenic mice in which IL-4 expression was augmented in developing T-lineage cells by coupling the IL-4 cDNA to the proximal promoter of the *lck* gene. Mice expressing the *lck*–IL-4 construct displayed perturbed T-cell development (11). Here we show that *lck*–IL-4 mice also developed severe osteoporosis primarily because of a profound decrease in osteoblast activity. These results demonstrate that IL-4 can have a dramatic negative influence on bone homeostasis *in vivo*.

MATERIALS AND METHODS

Mice. The generation of *lck*–IL-4 transgenic mice has been described (11).

Radiography. For conventional radiography, mice were anesthetized by intraperitoneal injection with ketamine/xyalazine and radiographed at 50 peak kilovoltage (kVp) for 0.5 sec, 100-mA station at a focal distance of 100 cm. For microradiography, mice were euthanized using CO_2; all necropsy tissue was immediately fixed in 10% (vol/vol) neutral-buffered formalin. Microradiographic exposures of fixed tissue were performed using high-resolution x-ray plates (type IA, Kodak) and a Hewlett–Packard Faxatron 805 unit at 100 kVp for 60 min at a focal distance of 60 cm. Microradiographs were then photographed with a Wild Heerbrugg M-400 Photomakroskop camera system using Tech-Pan film.

Biomechanical Studies and Micro-Computed Tomography. Whole-bone four-point bending tests to failure were conducted on a servo-hydraulic testing system at a constant displacement rate of 0.5 mm/sec (12, 13). Micro-computed tomography was used to quantify the cross-sectional radius, moment of inertia, and cortical thickness of a 2- to 3-mm mid-diaphyseal region of femur specimens (13). The scan region was divided into 20-μm sections, producing an average of 150 transverse sections for each femur. Images were thresholded to delineate each pixel as "bone" or "nonbone" (13).

Histologic Analysis. For routine histologic analysis, the caudal vertebrae and bones of the hindlimbs were fixed in formalin, decalcified in 10% Na_2EDTA (pH 6.9) and stained with hematoxylin and eosin. For histomorphometric analysis, mice received intraperitoneal injections of tetracycline as described (14). After necropsy, bone tissue was fixed in formalin, dehydrated in acetone, embedded in methylacrylate, sectioned, stained by the modified Masson method, and histomorphometrically analyzed (15). For enzymo-histochemical staining, bone tissue was fixed in 70% ethanol, decalcified in Na_2EDTA or formate acid/citrate buffer (pH 4.2), embedded in OCT freezing medium, frozen in liquid nitrogen-cooled isopentane, sectioned, and stained for either alkaline phosphatase (AP) activity or tartrate-resistant acid phosphatase (TRAP) (16).

Serum Assays. Total protein, calcium, phosphorus, and creatinine (10 μl per test) were determined using a Kodak

The publication costs of this article were defrayed in part by page charge payment. This article must therefore be hereby marked "*advertisement*" in accordance with 18 U.S.C. §1734 solely to indicate this fact.

Abbreviations: IL-4, interleukin 4; AP, alkaline phosphatase; TRAP, tartrate-resistant acid phosphatase; RT, reverse transcriptase; PTH, parathyroid hormone.

[c]To whom reprint requests should be addressed.

EktaChem 700XR analyzer. Osteocalcin content of sera was determined in duplicate using a commercial RIA kit (Biomedical Technologies, Stoughton, MA) by following the manufacturer's instructions.

Reverse Transcriptase (RT)–PCR. Total RNA was isolated from bone marrow cells, thymocytes, and phorbol 12-myristate 13-acetate-stimulated EL4 cells as described (11) and incubated for 45 min at 37°C with RQ1 RNase-free DNase (Promega; 80 units/ml) in 40 mM Tris·HCl, pH 7.5/7.5 mM $MgCl_2$/2.5 mM spermidine/10 mM dithiothreitol/placental RNasin (Promega; 1.5 units/μl). After heat inactivation of DNase, 2.5 μg of DNase-treated total RNA was assayed by RT–PCR as described (17) using random hexamers and murine moloney virus RT (GIBCO/BRL; 10 units/ml). As a negative control, RT was omitted. PCR was performed for 35 cycles (1 min at 94°C, 1 min at 59°C, and 2 min at 72°C), using *Taq* polymerase (Promega) and either murine IL-4 or β-actin primers (18) that amplify cDNA products of 180 and 348 bp, respectively. Reaction products (5 μl per lane) were electrophoresed in 1.5% agarose and stained in ethidium bromide. Electrophoresed IL-4 reaction products were blotted to nylon membranes (Micron Separations, Westboro, MA), hybridized with an internal ^{32}P-labeled DNA probe [nt 259–352 of the murine IL-4 cDNA sequence (19)], washed, and autoradiographed (11).

Statistics. Values are presented as the mean ± SEM. Probabilities of differences between transgenic and littermate control groups were determined using the unpaired two-tailed Student's *t* test unless otherwise indicated.

RESULTS

We observed that both sexes of one line of *lck*–IL-4 transgenic mice [line 1315 (11)] became progressively humpbacked, starting between 3 and 6 months after birth. Radiography revealed kyphosis, an exaggerated curvature of the spine (Fig. 1*A*), but no other signs of skeletal dysmorphism. Longitudinal growth occurred normally. Necropsied bones of *lck*–IL-4 mice of the 1315 line were semitranslucent, suggesting decreased bone mass. This abnormal skeletal appearance was invariably present in both transgenic females and males by 2 months of age and has remained stable during propagation of the 1315 line for 11 generations on a C57BL/6 genetic background. Microradiography revealed cortical thinning of the skeleton in *lck*–IL-4 mice, most striking in the long bones (Fig. 1 *B* and *C*). An analysis of four 3-month-old *lck*–IL-4 mice and four littermate controls demonstrated significant reduction in the mean cortical thickness and percent cortical area at the midshaft of the radius and ulna in the transgenic animals (data not shown). Bone disease was not explained by cachexia: The weights (mean ± SEM) for five 2-month-old male *lck*–IL-4 mice, all manifesting bone disease, and five male littermate controls were 23.5 ± 1.0 and 24.1 ± 0.4 g, respectively ($P = 0.64$).

IL-4 overexpression had a complex and dramatic influence on the mechanical properties and geometry of long bone *in vivo* (Table 1). Both the stiffness (a measure of elastic deformation) and failure load (a measure of whole-bone bending strength) were significantly reduced in *lck*–IL-4 specimens. The anterior–posterior cross-section of *lck*–IL-4 femur specimens was significantly increased relative to controls, but the medial-lateral cross-section showed only a strong trend toward a significant increase. Thus, *lck*–IL-4 specimens had an increased cross-section and tended to be more round than oval (Fig. 1*D*). These changes were not associated with a significant increase in the moment of inertia (a measure of the geometrical resistance to bending) because the cortex of *lck*–IL-4 specimens was significantly thinner than normal.

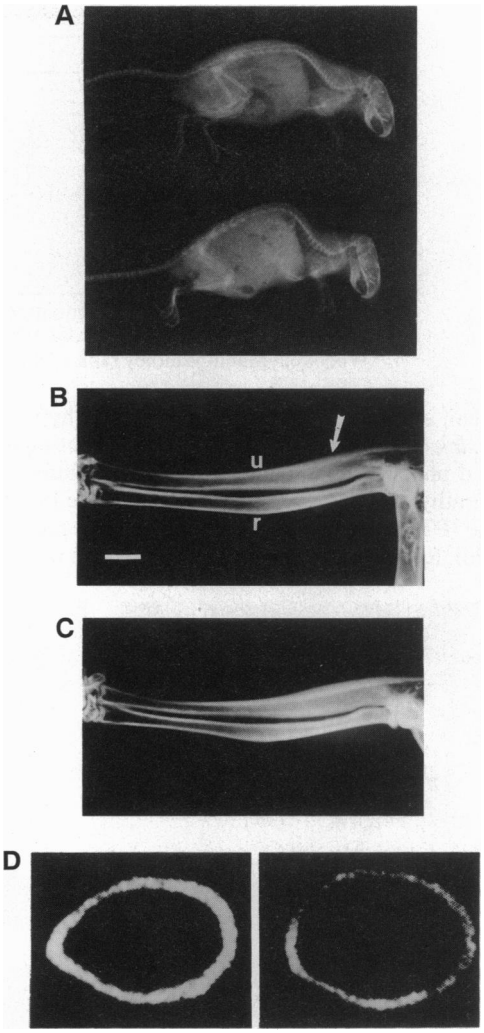

FIG. 1. Radiography and computed tomography of bone tissue. (*A*) Lateral radiograph of a live 3-month-old nontransgenic male (*Upper*) and a *lck*–IL-4 male mouse (*Lower*). Lateral microradiographs, at identical magnification, of the forelimb of a 3-month-old *lck*–IL-4 male mouse (*B*) and a nontransgenic male littermate (*C*). Marked cortical thinning of the ulna (arrow) and radius is evident in the transgenic mouse. (Bar = 1.25 mm.) r, Radius; u, ulna. Microcomputed tomographic transverse sections from the femoral midiaphysis of a 4-month-old female littermate control mouse (*Left*) and a *lck*–IL-4 female mouse (*Right*) (*D*). The tomographic images shown are representative of a 2- to 3-mm region at the mid-diaphysis.

Histologic analysis demonstrated substantially decreased cortical and trabecular mass in the vertebral bodies as well as long bones from transgenic animals. Importantly, these decreases were seen in bone tissue from an independently derived *lck*–IL-4 founder animal, 4475, in which the transgene had presumably integrated at a different site than for the 1315 line (Fig. 2 *A* and *B*). These results indicated that the bone disease phenotype observed in *lck*–IL-4 mice resulted from *lck*–IL-4 transgene expression rather than a mutation produced by transgene integration.

Histologic analysis did not reveal an excess of unmineralized matrix in *lck*–IL-4 bone tissue (Fig. 2 *A* and *B*), indicating that *lck*–IL-4 mice had an osteoporosis and not osteomalacia. Histologic and radiologic stigmata of other osteopenic disorders, including primary hyperparathyroidism and renal osteodystrophy, were also absent (data not shown). Transgenic and littermate-control animals had similar total serum calcium and protein levels (Table 2), indicating that serum-free calcium levels were probably normal in *lck*–IL-4 mice,

Table 1. Biomechanical (structural and geometrical) properties

Property	*lck*–IL-4	Control	*P* value
Structural			
Stiffness, N/mm	69.9 ± 2.5	105.2 ± 9.2	<0.01
Failure load, N	12.3 ± 1.5	17.1 ± 1.8	<0.01
Geometrical			
Radius (A–P), mm	0.62 ± 0.02	0.57 ± 0.01	<0.008
Radius (M–L), mm	0.85 ± 0.02	0.82 ± 0.02	<0.06
Moment of inertia, mm^4	0.084 ± 0.008	0.076 ± 0.003	<0.143
Cortical thickness, mm	0.124 ± 0.007	0.148 ± 0.007	<0.008

Results using femurs from 3-month-old *lck*–IL-4 ($n = 5$) and nontransgenic littermate ($n = 5$) females are shown. Statistical significance between *lck*–IL-4 and control values was determined by the Wilcoxon–Mann–Whitney rank sum test. N, newton(s); A–P, anterior–posterior; M–L, medial–lateral.

rather than elevated as is typical for primary hyperparathyroidism. *lck*–IL-4 sera also exhibited a small but significantly increased phosphate concentration. This excluded primary hyperparathyroidism since abnormally increased parathyroid hormone (PTH) secretion typically lowers serum phosphate levels (20). Renal insufficiency in *lck*–IL-4 mice was excluded by the normal serum creatinine (Table 2) and normal microscopic renal histology (data not shown).

Osteoblasts in *lck*–IL-4 bone tissue were markedly atrophic (Fig. 2 *C* and *D*). Consistent with this result, the proportion of bone surface lined by osteoblasts in *lck*–IL-4 mice of the 1315 line, as well as in the 4475 founder animal,

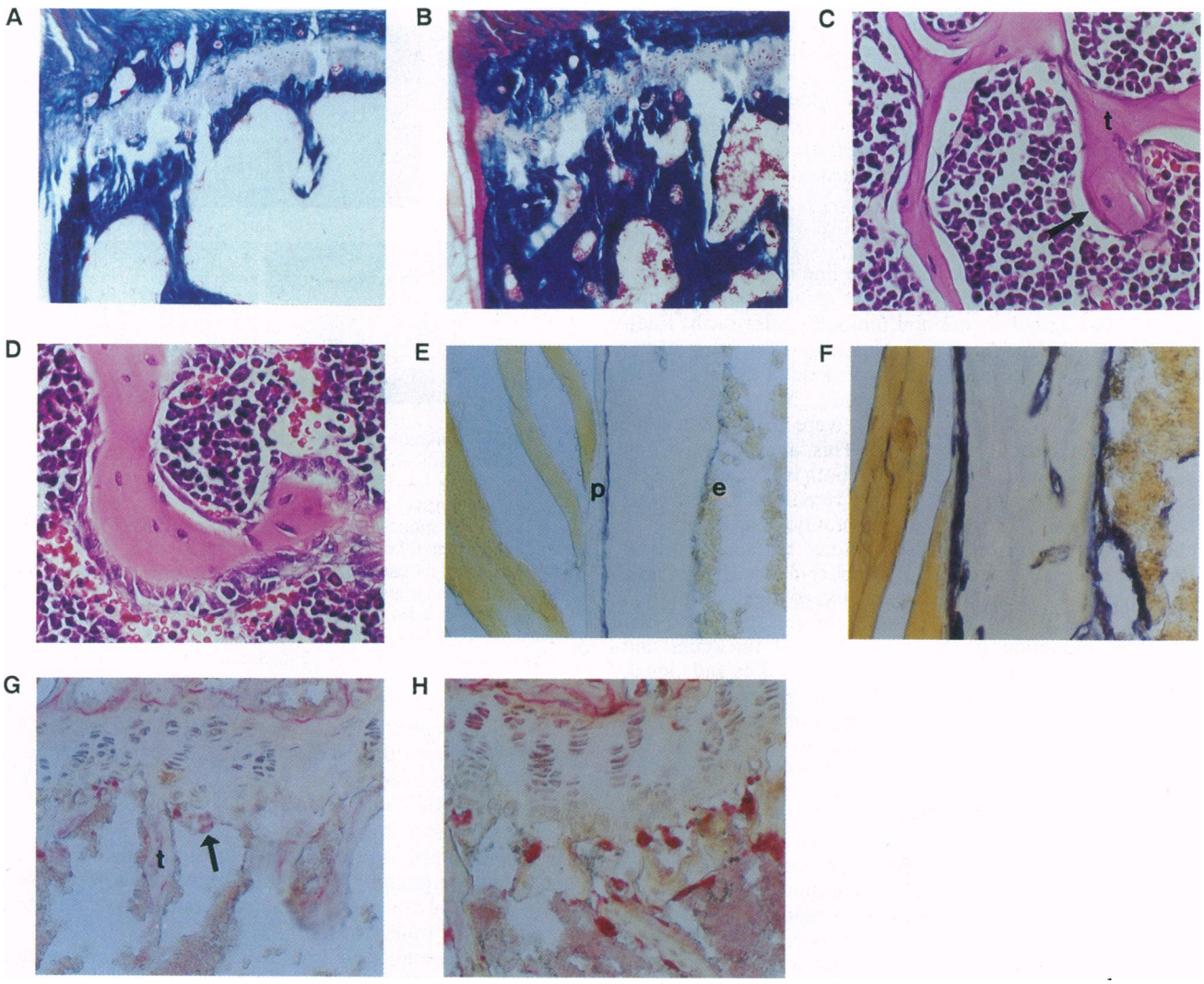

FIG. 2. Histologic analysis of bone tissue. (*A* and *B*) Sagittal section of a caudal vertebral body from the 9-month-old *lck*–IL-4 4475 founder mouse (*A*) and an age- and sex-matched C57BL/6J female control (*B*). (Modified Masson stain, ×30.) Marked reductions in cortical and trabecular bone mass are evident in the transgenic tissue. (*C* and *D*) Proximal tibial metaphysis from a 12-week-old *lck*–IL-4 1315 line mouse (*C*) or a nontransgenic littermate (*D*). (Hematoxylin and eosin stain, ×70.) Bone is stained pink. The thin trabeculae of *lck*–IL-4 bone tissue are lined by atrophic osteoblasts (arrow). (*E* and *F*) Tibiae from a 2-month-old *lck*–IL-4 female mouse (*E*) and a nontransgenic littermate (*F*) stained for AP. (×10.) A generalized and dramatic reduction in AP (blue stain) associated with *lck*–IL-4 osteoblasts of the periosteum and endosteum is seen. (*G* and *H*) Proximal tibial metaphysis of *lck*–IL-4 (*G*) and littermate control (*H*) mice stained for TRAP. (×30.) The arrow indicates an example of reduced TRAP staining by *lck*–IL-4 osteoclasts. e, Endosteum, p, periosteum; t, trabeculae.

Table 2. Serum components in 3-month-old adult *lck*–IL-4 and littermate control mice

Mouse	Total protein, g/dl	Ca^{2+}, mg/dl	Phosphorus, mg/dl	Creatinine, mg/dl	Osteocalcin, ng/ml
lck–IL-4	5.85 ± 0.05	10.0 ± 0.1	9.2 ± 0.3*	0.1 ± 0.0	84 ± 55*
Littermate control	5.70 ± 0.00	10.2 ± 0.2	8.1 ± 0.5	0.1 ± 0.0	162 ± 12

Results representative of two experiments are shown. Similar results were obtained when data from female or male mice were separately analyzed.
*$P < 0.05$ for *lck*–IL-4 vs. control values.

was <60% that of the control value (data not shown). Osteoblast biosynthetic function in *lck*–IL-4 mice was markedly decreased by several criteria. (*i*) Decreased levels of osteocalcin, a protein made exclusively by osteoblasts and odontoblasts (21), were invariably found in *lck*–IL-4 sera (Table 2). (*ii*) Profoundly decreased AP activity *in situ* was observed for osteoblasts lining the periosteum, endosteum, and trabeculae (Fig. 2 *E* and *F*). (*iii*) The percent of bone surface labeled *in vivo* was substantially reduced: In an experiment representative of results obtained with three litters, the percent total tetracycline surface for three 4-month-old *lck*–IL-4 mice and three littermate controls was 32.2 ± 3.7 and 49.0 ± 3.1, respectively ($P < 0.05$). These results characterize a state of decreased bone formation in the osteoporosis of *lck*–IL-4 mice.

Since IL-4 has been reported to inhibit *in vitro* osteoclastogenesis and osteoclast-mediated bone resorption (22), bone tissue from *lck*–IL-4 mice was analyzed for osteoclast number and function. The number of osteoclasts per mm^2 in the metaphyseal region of the tibia from four 3-month-old *lck*–IL-4 and three littermate controls was 2.75 ± 0.69 and 1.92 ± 0.05, respectively ($P = 0.37$), indicating that osteoclastogenesis probably occurred normally in transgenic animals. However, TRAP activity expressed by osteoclasts *in situ* was markedly reduced in *lck*–IL-4 bone tissue compared to osteoclasts in littermate control tissue (Fig. 2 *G* and *H*), suggesting that osteoclast function was altered in *lck*–IL-4 mice.

Bone tissue from *lck*–IL-4 mice was also specifically examined for mast cell infiltration, since IL-4 is a mast cell growth factor (23) and mastocytosis is a rare but well-documented cause of human osteoporosis (24). However, no mast cell infiltration of bone or soft tissues was found, indicating that mastocytosis did not mediate the bone disease of *lck*–IL-4 mice.

To determine whether a local action of IL-4 in mediating osteoporosis was plausible, bone marrow cells from transgenic mice and littermate controls were analyzed for expression of IL-4 mRNA. Constitutive expression of IL-4 mRNA in bone marrow cells of *lck*–IL-4 but not littermate controls was detectable by RT–PCR (Fig. 3*A*). Consistent with earlier studies (11), IL-4 mRNA was also found in freshly isolated thymocytes and splenocytes from transgenic mice but not littermate controls and was also detected in an IL-4-producing T-cell line, EL-4. Similar amounts of β-actin transcripts were detected in all RNA samples (Fig. 3*B*), indicating that differences in IL-4 transcript abundance did not reflect variation in the efficiency of the RT reaction. No IL-4 or β-actin PCR products were detected in any RNA samples, including bone marrow RNA, when RT was omitted (Fig. 3, lanes 8–11). Thus, the PCR products amplified from transgenic RNA samples did not reflect residual contaminating genomic DNA. These results suggest that the bone microenvironment of *lck*–IL-4 mice was exposed to higher levels of IL-4 than occur normally.

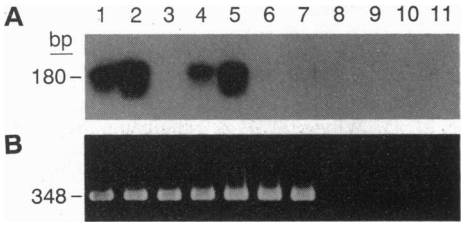

FIG. 3. RT–PCR for IL-4 and β-actin transcripts. The results shown are representative of two experiments using total cellular RNA from 3-month-old *lck*–IL-4 1315 line mice and nontransgenic littermates. (*A*) IL-4 sequences detected by Southern blot analysis. (*B*) β-Actin PCR products visualized by staining with ethidium bromide. Lanes 1–7 show PCR products obtained using total RNA from EL-4 cells (lane 1), thymocytes from an *lck*–IL-4 (lane 2) or nontransgenic littermate (lane 3), and bone marrow cells from individual *lck*–IL-4 (lanes 4 and 5) and nontransgenic littermate (lanes 6 and 7) mice. Lanes 8–11 show PCR products obtained using RNA from phorbol 12-myristate 13-acetate-treated EL-4 cells (lane 8), *lck*–IL-4 thymocytes (lane 9), and *lck*–IL-4 bone marrow cells (lanes 10 and 11), when RT was omitted.

DISCUSSION

lck–IL-4 mice of both sexes displayed a generalized form of osteoporosis without evidence of other osteopenic disorders, such as osteomalacia, hyperparathyroidism, or renal osteodystrophy. Cortical thinning of the degree that occurred in *lck*–IL-4 mice has also been reported in cases of human osteoporosis (25). The loss of trabecular bone in vertebral bodies, a particularly prominent feature in human involutional osteoporosis (2), was also observed in *lck*–IL-4 animals. Although spontaneous fractures were not observed among 12 *lck*–IL-4 mice examined radiographically, bone mechanical integrity was decreased in these transgenic animals.

Cortical thinning is often accompanied by increased cross-sectional geometry in individuals with osteoporosis (26) and was also observed in *lck*–IL-4 femur specimens. For *lck*–IL-4 femurs, the relationship between geometry and structural properties is complex because of the balancing effects of an increase in cross-section, a geometry that should increase mechanical properties, vs. a decrease in cortical thickness, which should decrease mechanical properties. Our data actually predict that *lck*–IL-4 specimens should have mechanical properties similar to controls (data not shown). However, the stiffness and failure load values for the transgenic specimens were significantly decreased (Table 1), which suggests that the material properties of *lck*–IL-4 specimens are altered by IL-4 overexpression.

Although kyphosis was a prominent feature of the phenotype of *lck*–IL-4 mice, it is not clear how this abnormality results from overexpression of IL-4. Kyphosis in osteopenic disorders is typically a secondary consequence of vertebral compression fractures, but such fractures were not observed in *lck*–IL-4 animals. It is possible that kyphosis may reflect increased deformability of the vertebral column as a result of osteopenia combined with alterations in the material properties of the remaining bone.

Based on the achievement of normal adult length, both primary bone formation and the activity of the growth plate appeared relatively unperturbed in *lck*–IL-4 mice. This suggests either that bone remodeling may be more sensitive than endochondral bone formation to negative effects mediated by

IL-4 or that IL-4-secreting cells accumulate with age in the bone marrow lymphoid compartment of *lck*–IL-4 mice. These possibilities are not mutually exclusive.

In an earlier study (11), IL-4 mRNA was undetectable in *lck*–IL-4 bone marrow cells using RNA blot analysis. Here, by using a more-sensitive PCR-based assay, constitutive expression of IL-4 mRNA was found in bone marrow cells from *lck*–IL-4 mice but not in bone marrow cells from nontransgenic littermates. Our finding of increased IL-4 mRNA within the bone marrow compartment of *lck*–IL-4 mice indicates that a locally mediated effect of IL-4 on bone homeostasis is plausible but does not exclude the possibility that increased IL-4 production could act indirectly to promote osteoporosis by altering the systemic production of hormones.

Decreased bone formation by osteoblasts appeared to be a major cause of osteoporosis in *lck*–IL-4 mice. Whether the transgene acts to decrease the activity of mature osteoblasts and/or inhibits the maturation of osteoblasts from less mature cells is unclear. The effect of IL-4 on osteoblasts could be mediated directly since osteoblast-lineage cells express functional IL-4 receptors and since IL-4 has been reported to inhibit the proliferation and expression of AP by a murine osteoblast cell line (27). IL-4 could compromise other biosynthetic functions mediated by osteoblasts, and it is known (12) that decreased production of type I collagen by osteoblasts can result in osteopenia, a form of osteogenesis imperfecta. However, the altered properties of *lck*–IL-4 specimens are not consistent with previous results obtained with the Mov13 murine model of osteogenesis imperfecta (12, 13): *lck*–IL-4 bone specimens showed decreased stiffness, whereas Mov13 specimens showed decreased plasticity in whole-bone bending tests to failure.

Our results indicate that the *lck*–IL-4 transgene does not significantly interfere with osteoclastogenesis, as has been observed *in vitro* (22). However, our finding of markedly decreased osteoclast-associated TRAP activity suggests that osteoclast function is altered in *lck*–IL-4 mice. If the resorption of bone by osteoclasts is, like osteoclast-associated TRAP activity, reduced in *lck*–IL-4 mice, then the osteoporosis presumably results from a more severe decrease in osteoblast function relative to osteoclast function.

The mechanism for the modest hyperphosphatemia in *lck*–IL-4 mice remains uncertain. Preliminary studies indicate that PTH levels are modestly elevated in *lck*–IL-4 mice (D.B.L., unpublished observations), possibly in response to this hyperphosphatemia. IL-4-induced osteopenia is also unlikely to be due to secondary elevation of PTH since hyperparathyroidism is associated with increased numbers and activity of osteoclasts and osteoblasts (28), the opposite of our findings in *lck*–IL-4 mice. Our results do not exclude the possibility that the skeletal tissue of *lck*–IL-4 mice may be resistant to the effects of PTH.

Regardless of the precise mechanism by which the *lck*–IL-4 transgene acts to induce osteoporosis, the *lck*–IL-4 mouse may facilitate the evaluation of potential therapies to prevent or ameliorate bone loss. Intriguingly, osteoporosis is a common complication in patients with the hyper-IgE syndrome, a heritable immunodeficiency in which B lymphocytes function as if exposed to excess IL-4 (29). Viewed in the context of the severe osteoporosis that develops in *lck*–IL-4 mice, this suggests that abnormalities in IL-4 production and/or IL-4-mediated signaling may alter osteoblast function and produce certain forms of human bone disease.

We thank Mary McGurn for assistance in performing the RT–PCR assays. This work was supported in part by grants from the National Institutes of Health (D.B.L., H.D.L., S.L.T., S.A.G., and J.B.), the March of Dimes (D.B.L.), and the Shriner's Hospital (S.L.T.) and by the Howard Hughes Medical Institute (R.M.P.).

1. Parfitt, A. M. (1984) *Calcif. Tissue Int.* **36**, Suppl. 1, S37–S45.
2. Riggs, B. L. & Melton, L. J., III (1986) *N. Engl. J. Med.* **327**, 620–627.
3. Avioli, L. V. (1991) *Calcif. Tissue Int.* **49**, Suppl. 1, S5–S7.
4. Gowen, M., Wood, D. D., Ihrie, E. J., McGuire, M. & Russell, R. G. G. (1983) *Nature (London)* **313**, 378–380.
5. Ishimi, Y., Miyaura, C., Jin, C. H., Akatsu, T., Abe, E., Nakamura, Y., Yamaguchi, A., Yoshiki, S., Matsuda, T., Hirano, T., Kishimoto, T. & Suda, T. (1990) *J. Immunol.* **145**, 3297–3303.
6. Bertolini, D. R., Nedwin, G. E., Bringman, T. S., Smith, D. D. & Mundy, G. R. (1986) *Nature (London)* **319**, 516–518.
7. Jilka, R. L., Hangoc, G., Giraole, G., Passeri, G., Williams, D. C., Abrams, J. S., Boyce, B., Broxmeyer, H. & Manolagas, S. C. (1992) *Science* **257**, 88–91.
8. Pacifici, R., Rifas, L., Teitelbaum, S., Slatopolsky, E., McCracken, R., Bergfeld, M., Lee, W., Avioli, L. V. & Peck, W. A. (1987) *Proc. Natl. Acad. Sci. USA* **84**, 4616–4620.
9. Pacifici, R., Brown, C., Puscheck, E., Friedrich, E., Slatopolsky, E., Maggio, D., McCracken, R. & Avioli, L. V. (1991) *Proc. Natl. Acad. Sci. USA* **88**, 5134–5138.
10. Paul, W. E. (1991) *Blood* **77**, 1859–1870.
11. Lewis, D. B., Yu, C. C., Forbush, K. A., Carpenter, J., Sato, T. A., Grossmann, A., Liggitt, D. A. & Perlmutter, R. M. (1991) *J. Exp. Med.* **173**, 89–100.
12. Bonadio, J., Saunders, T. L., Tsai, E., Goldstein, S. A., Morris-Wiman, J., Brinkley, L., Dolan, D. F., Altschuler, R. A., Hawkins, J. E., Jr., Bateman, J. F., Mascara, T. & Jaenisch, R. (1990) *Proc. Natl. Acad. Sci. USA* **87**, 7145–7149.
13. Bonadio, J., Jepsen, K., Mansoura, M. K., Kuhn, J. L., Goldstein, S. A. & Jaenisch, R. (1993) *J. Clin. Invest.* **92**, 1697–1705.
14. Marie, P. J., Hott, M. & Garba, M.-T. (1985) *Metabolism* **34**, 777–783.
15. Whyte, M. P., Bergfeld, M. A., Murphy, W. A., Avioli, L. V. & Teitelbaum, S. L. (1982) *Am. J. Med.* **72**, 193–202.
16. Liu, C., Sanghvi, R., Burnell, J. M. & Howard, G. A. (1987) *Histochemistry* **86**, 559–565.
17. Van Voorhis, W. C. (1992) *J. Immunol.* **148**, 239–248.
18. Murray, L. J., Lee, K. & Martens, C. (1990) *Eur. J. Immunol.* **20**, 163–170.
19. Noma, Y., Sideras, P., Naito, T., Bergstedt-Lindquist, S., Azuma, C., Severinson, E., Tanabe, T., Kinashi, T., Matsuda, F., Yaoita, Y. & Honjo, T. (1986) *Nature (London)* **319**, 640–646.
20. Robey, P. G. (1989) *Endocrin. Metabol. Clin. N. Am.* **18**, 859–902.
21. Price, P. A., Parthemore, J. G. & Deftos, L. J. (1980) *J. Clin. Invest.* **66**, 878–883.
22. Shioi, A., Teitelbaum, S. L., Ross, F. P., Welgus, H. G., Ohara, J., Suzuki, H. & Lacey, D. L. (1991) *J. Cell. Biochem.* **47**, 272–277.
23. Brown, M. A., Pierce, J. H., Watson, C. J., Falco, J., Ihle, J. N. & Paul, W. E. (1987) *Cell* **50**, 809–818.
24. Fallon, M. D., Whyte, M. P. & Teitelbaum, S. L. (1981) *Hum. Pathol.* **12**, 813–819.
25. Garn, S. M., Poznanski, A. K. & Nagy, J. M. (1971) *Radiology* **100**, 509–518.
26. Martin, R. B. & Atkinson, P. J. (1977) *J. Biomech.* **10**, 223–231.
27. Lacey, D. L., Erdmann, J. M., Suzuki, H. & Ohara, J. (1991) *J. Bone Miner. Res.* **6**, S255.
28. Reeve, J., Meunier, P. J., Parsons, J. A., Bernat, M., Bijvoet, O. L. M., Corupron, P., Edouard, C., Klenerman, L., Neer, R. M., Renier, J. C., Slovik, D., Vismans, F. J. F. E. & Potts, J. T. (1980) *Br. Med. J.* **2**, 1340–1344.
29. Leung, D. Y. & Geha, R. S. (1988) *Hematol. Oncol. Clin. N. Am.* **2**, 81–100.